Electrochimica Acta 174 (2015) 1185–1191

Contents lists available at ScienceDirect

Electrochimica Acta

journal homepage: www.elsevier.com/locate/electacta

Al_2O_3 Coated Concentration-Gradient $Li[Ni_{0.73}Co_{0.12}Mn_{0.15}]O_2$ Cathode Material by Freeze Drying for Long-Life Lithium Ion Batteries

Jingpeng Wang[a], Chunyu Du[a,*], Chunqiu Yan[a], Xiaoshu He[a], Bai Song[b], Geping Yin[a], Pengjian Zuo[a], Xinqun Cheng[a]

[a] School of Chemical Engineering and Technology, Harbin Institute of Technology, Harbin 150001, China
[b] Harbin Coslight Power Co., FD., No.8 Taihu South Street, Harbin 150060, China

ARTICLE INFO

Article history:
Received 24 March 2015
Received in revised form 1 June 2015
Accepted 23 June 2015
Available online 29 June 2015

Keywords:
lithium ion battery
nickel-rich cathode material
concentration gradient shell
Al_2O_3 coating
freeze drying

ABSTRACT

In order to enhance the electrochemical performance of the high capacity layered oxide cathode with a Ni-rich core and a concentration-gradient shell (NRC-CGS), we use a freeze drying method to coat Al_2O_3 layer onto the surface of NRC-CGS $Li[Ni_{0.73}Co_{0.12}Mn_{0.15}]O_2$ material. The samples are characterized by X-ray diffraction, scanning electron microscopy, transmission electron microscopy, charge-discharge measurements and electrochemical impedance spectroscopy. It is revealed that an amorphous Al_2O_3 layer of about 5 nm in thickness is uniformly formed on the surface of NRC-CGS $Li[Ni_{0.73}Co_{0.12}Mn_{0.15}]O_2$ material by the freeze drying procedure. The freeze drying Al_2O_3-coated (FD-Al_2O_3-coated) sample demonstrates similar discharge capacity and significantly enhanced cycling performances, in comparison to the pristine and conventional heating drying Al_2O_3-coated (HD-Al_2O_3-coated) samples. The capacity decay rate of FD-Al_2O_3-coated $Li[Ni_{0.73}Co_{0.12}Mn_{0.15}]O_2$ material is 1.7% after 150 cycles at 55 °C, which is 9 and 12 times lower than that of the pristine and HD-Al_2O_3-coated samples. The superior electrochemical stability of the FD-Al_2O_3-coated sample is attributed to the synergistic protection of CGS and high-quality Al_2O_3 coating that effectively protect the active material from electrolyte attack. The freeze drying process provides an effective method to prepare the high performance surface-coated electrode materials.

1. Introduction

Rechargeable lithium ion batteries (LIBs) have attracted a great deal of attention as power sources for portable electronic devices, electric vehicles (EVs) or hybrid electric vehicles (HEVs), due to their high energy and power density, wide operation temperature range and long cycling life [1,2]. The development of rechargeable LIBs is mainly determined by the cathode materials, which dominate the cost, energy and power density, safety and working life of LIBs. Nickel-rich $Li[Ni_xCo_yMn_{1-x-y}]O_2$ ($x \geq 0.6$) layered oxides are among the most promising cathode materials because of their relatively low cost, low toxicity, high rate capability and excellent reversible capacity [3,4]. However, highly delithiated nickel-rich $Li[Ni_xCo_yMn_{1-x-y}]O_2$ materials become unstable due to the appearance of abundant Ni^{4+} ions, which react with organic electrolyte, increasing the impedance and lowering the cyclability of LIBs. Meanwhile, the delithiated $Li[Ni_xCo_yMn_{1-x-y}]O_2$ materials decompose exothermally around 200 °C, and release oxygen from the host structure, which reacts with the organic electrolyte to cause severe thermal runaway and safety problems [5,6]. Therefore, the application of nickel-rich $Li[Ni_xCo_yMn_{1-x-y}]O_2$ oxides is significantly limited by the undesirable cycling performance, poor thermal stability and increased impedance during cycling, particularly at elevated temperatures.

Recently, Sun et al. have developed a novel concept of core-shell cathode materials with a nickel-rich core and a concentration-gradient shell (NRC-CGS) [6,7]. The nickel-rich core delivers high reversible capacity, whereas the nickel-poor shell provides high thermal and cycling stability. Therefore, the NRC-CGS $Li[Ni_xCo_yMn_{1-x-y}]O_2$ materials exhibit promising electrochemical performance for LIBs [8,9]. However, due to the oxidation of nickel in the charging process, Ni^{4+} is still present in the outermost surface of the NRC-CGS materials, which will react with the electrolyte, leading to undesirable capacity fading, especially at elevated temperatures.

Another promising approach to improving the thermal stability and cyclability of the Ni-rich $Li[Ni_xCo_yMn_{1-x-y}]O_2$ materials is to

* Corresponding author at: Chunyu Du School of Chemical Engineering and Technology, Harbin Institute of Technology, Harbin 150001, China. Tel.: +86 451 86403961; Fax: +86 451 86418616.
E-mail address: cydu@hit.edu.cn (C. Du).

http://dx.doi.org/10.1016/j.electacta.2015.06.112
0013-4686/

coat those materials with a thin layer of inactive compounds [10,11]. Various surface modification compounds [12–23], such as Al_2O_3, $AlPO_4$ and AlF_3, have been reported. These coated materials present significantly improved cycling stability, rate capability and thermal stability compared to the corresponding pristine materials. The improvements are mainly attributed to stabilizing the host structure against HF attack and reducing the reaction between the electrode and the electrolyte, leading to the stable interface during extensive cycling [10,12,23]. Unfortunately, the conventional wet chemistry coating methods using heat evaporation of solvent are difficult to control the thickness, composition, uniformity and conformity of the coatings. Although the atomic layer deposition approach is able to grow conformal ultrathin coatings on the electrode materials, the high cost, complexity and strict requirements for precursors limit its large scale application. Therefore, a facile, low-cost, high-efficiency and up-scalable coating method is still a significant technical challenge.

In this paper, we coat a thin and uniform Al_2O_3 layer onto a NRC-CGS $Li[Ni_xCo_yMn_{1-x-y}]O_2$ cathode material with the average chemical composition of $Li[Ni_{0.73}Co_{0.12}Mn_{0.15}]O_2$, by using a freeze drying method. This drying method prevents the material from further damage in the solvent evaporation process through reducing the temperature. Furthermore, the solvent evaporation rate, which is proportional to temperature, has a significant impact on the flowability of coating precursor. The reduced solvent evaporation rate due to the freezing temperature is beneficial to promoting the surface-tension-gradient-induced leveling of the coating precursor [24], generating the uniform Al_2O_3 coating layer. Thus-obtained Al_2O_3-coated $Li[Ni_{0.73}Co_{0.12}Mn_{0.15}]O_2$ material (denoted as FD-Al_2O_3-coated $Li[Ni_{0.73}Co_{0.12}Mn_{0.15}]O_2$) is characterized by X-ray diffraction (XRD), scanning electron microscopy (SEM), transmission electron microscopy (TEM), charge-discharge measurements and electrochemical impedance spectroscopy (EIS). For the sake of comparison, the Al_2O_3-coated $Li[Ni_{0.73}Co_{0.12}Mn_{0.15}]O_2$ material is prepared by conventional heat drying method (denoted as HD-Al_2O_3-coated $Li[Ni_{0.73}Co_{0.12}Mn_{0.15}]O_2$). The FD-$Al_2O_3$-coated $Li[Ni_{0.73}Co_{0.12}Mn_{0.15}]O_2$ material has a Ni-rich $LiNi_{0.8}Co_{0.1}Mn_{0.1}O_2$ core that delivers high capacity of over 185 mAh g^{-1}, and a combination of CGS shell and uniform Al_2O_3 coating that synergistically protect the material from electrolyte, so that this material shows enhanced cyclability over the pristine and HD-Al_2O_3-coated $Li[Ni_{0.73}Co_{0.12}Mn_{0.15}]O_2$ materials at both room and elevated temperatures. To the best of our knowledge, this is the first report on the surface-coated NRC-CGS Li $[Ni_xCo_yMn_{1-x-y}]O_2$ cathode materials so far, which can be considered as a very promising electrode material applied to the elevated temperature environments. Our freeze drying strategy can be potentially applied to various surface coatings of electrode materials.

2. Experimental

The spherical $[Ni_{0.73}Co_{0.12}Mn_{0.15}](OH)_2$ precursor with Ni-rich $[Ni_{0.8}Co_{0.1}Mn_{0.1}](OH)_2$ core and Ni-poor CGS, whose surface composition was $[Ni_{0.4}Co_{0.2}Mn_{0.4}](OH)_2$, was synthesized through a co-precipitation reaction using aqueous solutions of $NH_3{\cdot}H_2O$, NaOH, $NiSO_4$, $CoSO_4$ and $MnSO_4$ at pH of 11.0 under a N_2 atmosphere according to the previously reported procedure [9]. After filtering, washing and drying at 110 °C for 12 h, the NRC-CGS $[Ni_{0.73}Co_{0.12}Mn_{0.15}](OH)_2$ precursor was mixed with a stoichiometric amount of $LiOH{\cdot}H_2O$, preheated at 480 °C for 5 h and then calcined at 750 °C for 20 h to obtain the spherical NRC-CGS Li $[Ni_{0.73}Co_{0.12}Mn_{0.15}]O_2$ product. To prepare Al_2O_3-coated NRC-CGS $Li[Ni_{0.73}Co_{0.12}$ -$Mn_{0.15}]O_2$ material, 10.0 g pristine $Li[Ni_{0.73}C$-$o_{0.12}Mn_{0.15}]O_2$ powder was mixed with ethanolic solution of isopropanol aluminum and vigorously stirred for 2 h. The ethanol solvent was subsequently removed via freeze drying (−45 °C) and heating drying (80 °C), respectively, and thus obtained powder was fired at 600 °C for 3 h in O_2 flow.

The crystalline phase of resulting samples was characterized by powder XRD using a Rigaku D/max-rA diffractometer with Cu Kα radiation. The morphology and structure of the samples were determined by SEM on a JEM 100CX-II microscope equipped with an energy dispersion X-ray spectroscopy (EDX) device at 20 kV, and TEM using a Hitachi model H-800 system operating at 150 kV. Cross-sections of the sample particles for EDX analysis were prepared by embedding the as-synthesized sample particles in an epoxy and then grinding them on metallographic sand papers. Elemental analysis was performed by inductively coupled plasma mass spectrometry (ICP-MS) using an Optima 5300DV instrument (Perkin Elmer).

The electrochemical performance of the pristine and Al_2O_3-coated NRC-CGS $Li[Ni_{0.73}Co_{0.12}Mn_{0.15}]O_2$ samples was tested using a CR2025-type coin cell. To prepare the working electrodes, the active material powder, Super-P conductive carbon black and poly (vinylidenefluoride) binder were mixed at a weight ratio of 80:10:10 in N-methyl-2-pyrrolidone solvent. The mixed viscous slurry was cast onto Al foil and dried at 120 °C under vacuum for 10 h. The obtained film was cut into circular discs with area of 1.5 cm^2, which were then pressed at a pressure of 10.0 MPa to use as the working electrodes. The working electrodes with about 2.5 mg active materials were assembled in coin cells with a lithium metal foil as the counter electrode, a Celgard 2400 film as the separator, and 1.0 M $LiPF_6$ solution in ethylene carbonate, diethyl carbonate and dimethyl carbonate (1:1:1 in volume) as the electrolyte. The charge/discharge behavior and cycling performance of the cells were tested using a NEWARE battery-testing system (Neware Co., FD., China) between 3.0 V and 4.3 V by applying constant current densities. The specific capacity was reported with respect to the total weight of pristine or Al_2O_3-coated active materials. EIS was measured on PARSTAT 2273 (Princeton Applied Research, USA). The amplitude of the AC signal was 5 mV over the frequency range between 100 kHz and 0.01 Hz. All the electrochemical measurements were carried out at room (25 °C) and elevated (55 °C) temperatures, and the potentials were reported with respect to Li^+/Li.

3. Results and discussion

XRD patterns of the pristine, HD-Al_2O_3-coated and FD-Al_2O_3-coated NCR-GCS $Li[Ni_{0.73}Co_{0.12}Mn_{0.15}]O_2$ materials are shown in

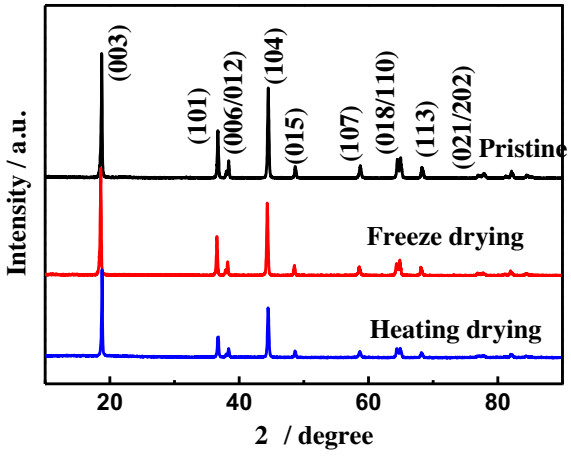

Fig. 1. X-ray diffraction patterns of the pristine, FD-Al_2O_3-coated and HD-Al_2O_3-coated $Li[Ni_{0.73}Co_{0.12}Mn_{0.15}]O_2$ materials.

Table 1
Lattice parameters of the pristine, FD-Al_2O_3-coated and HD-Al_2O_3-coated Li$[Ni_{0.73}Co_{0.12}Mn_{0.15}]O_2$ materials.

	a (Å)	c (Å)	I_{003}/I_{104}(R)
$Li[Ni_{0.73}Co_{0.12}Mn_{0.15}]O_2$	2.8695	14.2013	1.21
FD-Al_2O_3-coated $Li[Ni_{0.73}Co_{0.12}Mn_{0.15}]O_2$	2.8745	14.2248	1.23
HD-Al_2O_3-coated $Li[Ni_{0.73}Co_{0.12}Mn_{0.15}]O_2$	2.8691	14.2127	1.20

Fig. 1. All the diffraction peaks for the pristine $Li[Ni_{0.73}Co_{0.12}Mn_{0.15}]O_2$ material can be indexed to a layered hexagonal α-$NaFeO_2$ structure (space group R-−3m\). The XRD pattern for the FD-Al_2O_3-coated and HD-Al_2O_3-coated $Li[Ni_{0.73}Co_{0.12}Mn_{0.15}]O_2$ materials is similar to that of the pristine sample, and no any phase ascribed to impurity and Al_2O_3 can be observed, implying that both the Al_2O_3 coating processes do not change the crystalline structure of the NCR-GCS $Li[Ni_{0.73}Co_{0.12}Mn_{0.15}]O_2$ material and the Al_2O_3 layer is amorphous or nano-sized. The lattice parameters of the pristine, FD-Al_2O_3-coated and HD-Al_2O_3-coated $Li[Ni_{0.73}Co_{0.12}Mn_{0.15}]O_2$ materials are calculated by the Rietveld refinement and summarized in Table 1. The lattice parameters of the FD-Al_2O_3-coated and HD-Al_2O_3-coated $Li[Ni_{0.73}Co_{0.12}Mn_{0.15}]O_2$ are close to those of the pristine material. The integrated intensity ratio (R) of the (0 0 3) to (1 0 4) peaks in the XRD patterns of layered oxides is a measurement of the cation mixing between Li^+ and Ni^{2+}, and a value of $R > 1.2$ is an indication of effectively restrained cation mixing [25]. The R value of the Al_2O_3-coated material is almost identical to that of the pristine material, illustrating that the crystal structure of the $Li[Ni_{0.73}Co_{0.12}Mn_{0.15}]O_2$ material is stable during the Al_2O_3-coating processes.

Fig. 2a presents SEM image of the pristine NRC-CGS $Li[Ni_{0.73}Co_{0.12}Mn_{0.15}]O_2$ material. This material has well-dispersed spherical shape with the average particle size of approximately 12 μm, and each spherical particle is made up of numerous primary grains of 100-200 nm that are aggregated. After the surface modification of $Li[Ni_{0.73}Co_{0.12}Mn_{0.15}]O_2$ material with Al_2O_3 (Fig. 2b and c), the morphology of the two samples are rather similar to that of the pristine sample, suggesting that the thickness of Al_2O_3 layer is thin and the Al_2O_3 modification processes are mild. The composition of the pristine $Li[Ni_{0.73}Co_{0.12}Mn_{0.15}]O_2$ material is examined by a cross-sectional linear scanning EDX as shown in Fig. 2d. The Ni, Co and Mn molar ratio of ~8:1:1 is maintained constant throughout the core. The thickness of the outer shell is approximately 1 μm, where the Mn and Co molar ratios increase linearly to ~0.4 and ~0.2, respectively, whereas the Ni ratio decreases to ~0.4. The composition of the pristine $Li[Ni_{0.73}Co_{0.12}Mn_{0.15}]O_2$ material is consistent with the designed values, indicating that the NRC-CGS $Li[Ni_{0.73}Co_{0.12}Mn_{0.15}]O_2$ material has been successfully synthesized. Fig. 2e shows the elemental mapping of Al, O, Ni, Co and Mn of a FD-Al_2O_3-coated NRC-CGS $Li[Ni_{0.73}Co_{0.12}Mn_{0.15}]O_2$ particle. The Al content in the FD-Al_2O_3-coated NRC-CGS $Li[Ni_{0.73}Co_{0.12}Mn_{0.15}]O_2$ material is 2 wt% by ICP-MS analysis (Table 2), which agrees well with the theoretic value. Moreover, an amount of Al element is present on the surface and no Al element is found in the center of the particle, demonstrating that Al_2O_3 layer has been coated on the surface of NRC-CGS $Li[Ni_{0.73}Co_{0.12}Mn_{0.15}]O_2$ material by the freeze drying method.

Fig. 3 shows TEM and high resolution TEM images of the pristine, FD-Al_2O_3-coated and HD-Al_2O_3-coated $Li[Ni_{0.73}Co_{0.12}Mn_{0.15}]O_2$ materials. The pristine material shows a very smooth edge line without any layer on the surface (Fig. 3a). For the FD-Al_2O_3-coated material (Fig. 3b), there seems a uniform and indistinct coating layer covered on the surface. However, some Al_2O_3 nanoparticles aggregate and are non-uniformly coated on the surface of the HD-Al_2O_3-coated material (Fig. 3c), verifying that the conventional heat drying is disadvantageous to control the thickness and uniformity of the coatings. For the pristine $Li[Ni_{0.73}Co_{0.12}Mn_{0.15}]O_2$ material (Fig. 3d), the neighboring lattice fringes have an approximate d-spacing value of 0.488 nm, which corresponds to the (0 0 3) plane of the hexagonal layered phase, consistent with the XRD result. For the FD-Al_2O_3-coated material (Fig. 3e), the coating layer has a uniform thickness of about 5 nm

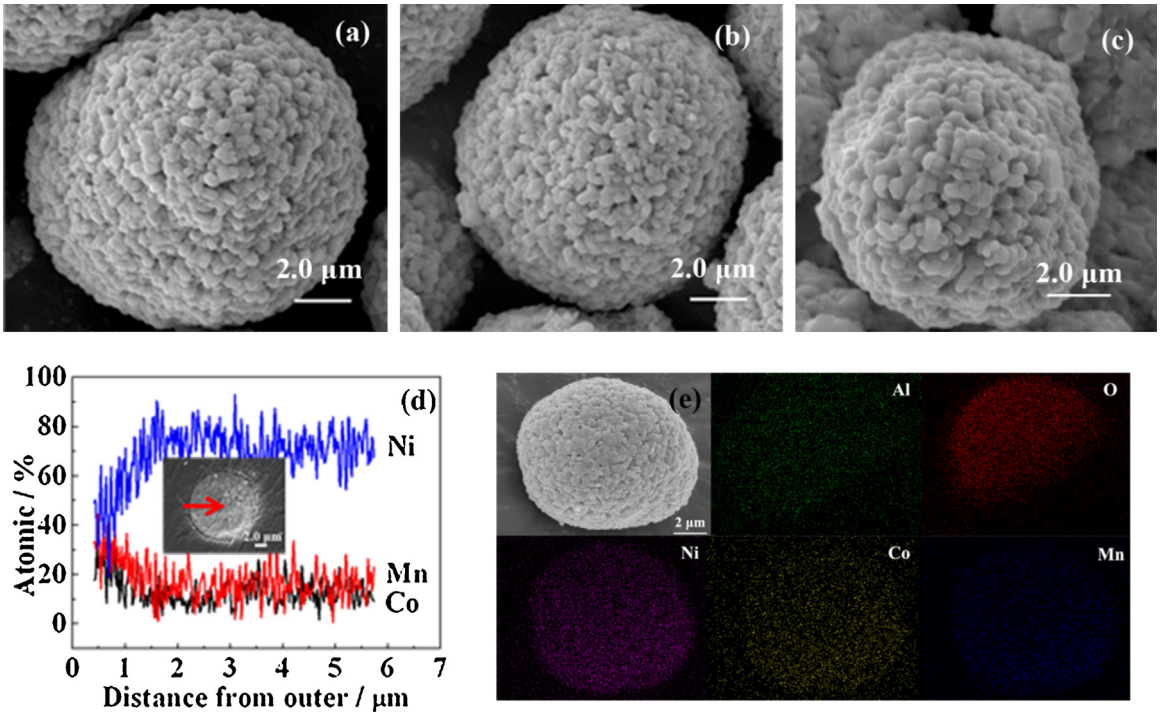

Fig. 2. SEM image of the pristine (a), FD-Al_2O_3-coated (b) and HD-Al_2O_3-coated (c) $Li[Ni_{0.73}Co_{0.12}Mn_{0.15}]O_2$ materials, cross-sectional EDX result of the pristine $Li[Ni_{0.73}Co_{0.12}Mn_{0.15}]O_2$ (d), and elemental mapping of Al, O, Ni, Co and Mn for the FD-Al_2O_3-coated $Li[Ni_{0.73}Co_{0.12}Mn_{0.15}]O_2$ material (e).

Table 2
Elemental analysis of the pristine, FD-Al_2O_3-coated and HD-Al_2O_3-coated $Li[Ni_{0.73}Co_{0.12}Mn_{0.15}]O_2$ materials by ICP.

	Content (molar ratio)				
	Li/(Ni + Co + Mn)	Ni	Co	Mn	Al (wt%)
$Li[Ni_{0.73}Co_{0.12}Mn_{0.15}]O_2$	1.015	0.732	0.119	0.149	0
FD-Al_2O_3-coated $Li[Ni_{0.73}Co_{0.12}Mn_{0.15}]O_2$	1.013	0.730	0.119	0.151	2.03
HD-Al_2O_3-coated $Li[Ni_{0.73}Co_{0.12}Mn_{0.15}]O_2$	1.012	0.728	0.121	0.151	2.02

and seems in porous and amorphous nature. This TEM analysis demonstrates that the freeze drying is an effective way to uniformly coat oxide layers on the cathode materials.

Fig. 4a illustrates the initial charge/discharge curves of the cells with the pristine, FD-Al_2O_3-coated and HD-Al_2O_3-coated NRC-CGS $Li[Ni_{0.73}Co_{0.12}Mn_{0.15}]O_2$ materials as cathodes at a current rate of 0.1 C (1 C = 200 mA g^{-1}) between 3.0 and 4.3 V vs Li/Li^+. All the cells show similar charge/discharge curves, indicating that the Al_2O_3 coatings do not cause noticeable changes of the bulk Li $[Ni_{0.73}Co_{0.12}Mn_{0.15}]O_2$ material. The initial charge and discharge capacities of the FD-Al_2O_3-coated $Li[Ni_{0.73}Co_{0.12}Mn_{0.15}]O_2$ material are 214 mAh g^{-1} and 186 mAh g^{-1}, respectively, which are slightly lower than those of the pristine $Li[Ni_{0.73}Co_{0.12}Mn_{0.15}]O_2$ material (226 mAh g^{-1} for charge and 191 mAh g^{-1} for discharge). This result is consistent with the fact that an inactive Al_2O_3 coating layer on the surface of $Li[Ni_{0.73}Co_{0.12}Mn_{0.15}]O_2$ particle usually leads to a slight capacity loss. However, the capacities of the FD-Al_2O_3-coated material are much higher than those of the HD-Al_2O_3-coated Li $[Ni_{0.73}Co_{0.12}Mn_{0.15}]O_2$ material (192 mAh g^{-1} for charge and 172 mAh g^{-1} for discharge), suggesting that the Al_2O_3 coating by freeze drying is beneficial to the Li^+ insertion/extraction in comparison with that by conventional heating drying.

Fig. 4b shows the differential capacity (dQ/dV) versus voltage profiles of the cells with pristine, FD-Al_2O_3-coated and HD-Al_2O_3-coated $Li[Ni_{0.73}Co_{0.12}Mn_{0.15}]O_2$ cathodes. For all the three cells, the peaks at different potential in the lithium extraction process are related to the first-order phase transition and one phase transition, of which the transition process is from hexagonal (R1) to monoclinic (M) phase (3.7∼3.9 V), and then to hexagonal (R2) phase (4.1∼4.3 V) [26]. In the charging (lithium extraction process) process, FD-Al_2O_3 coated material causes the cells an increase of the onset potential (from 3.68 of the pristine to 3.72 V) and the peak intensity. Whereas, that of HD-Al_2O_3 coated material is consistent with the pristine material. Thus it can be suggested that the Al ions doped into the host material plays the suppression role. The possible reason for this suppression is that the Al ions doped into the surface regions of the host $Li[Ni_{0.73}Co_{0.12}Mn_{0.15}]O_2$ material increases the metal–oxygen bond energy to a higher level due to the stronger Al—O bond which enhances the structural stability of the material compared with the Ni—O, Mn—O or Co—O bond [27]. Therefore, it could be concluded that FD-Al_2O_3 coated method improves the electrochemical properties and the structural stability of the materials.

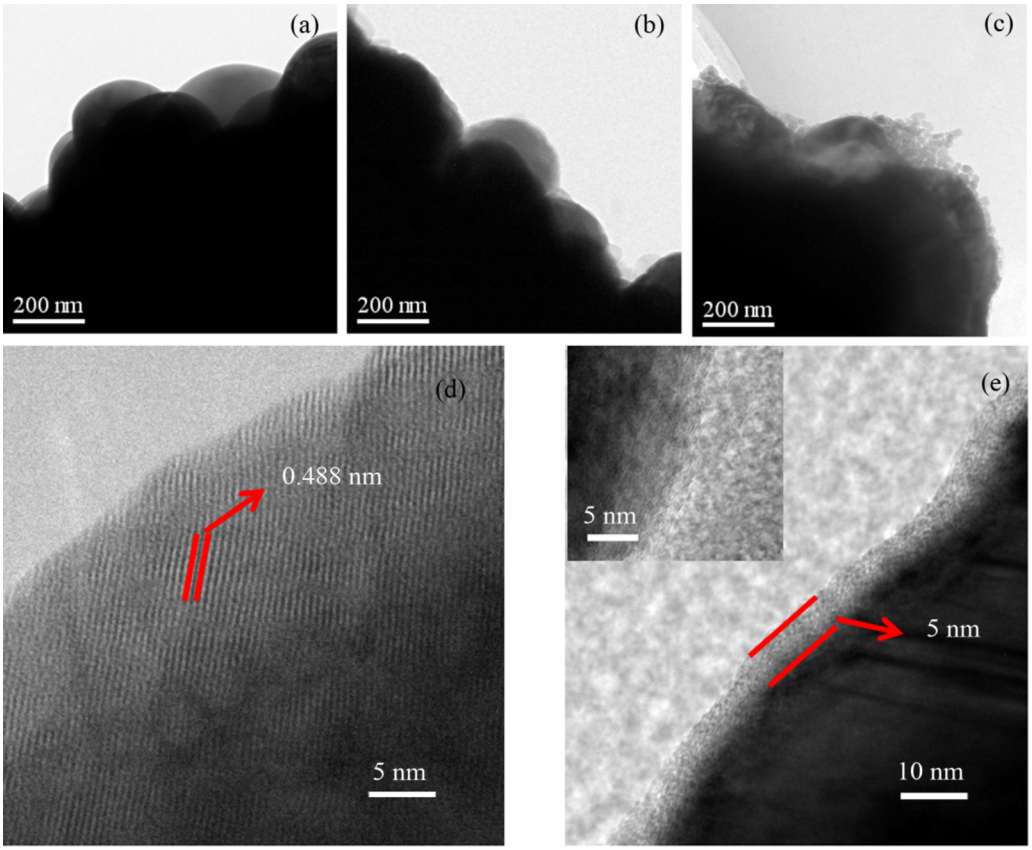

Fig. 3. TEM images of the pristine (a), FD-Al_2O_3-coated (b) and HD-Al_2O_3-coated (c) $Li[Ni_{0.73}Co_{0.12}Mn_{0.15}]O_2$ materials, and high resolution TEM images of the pristine (d) and FD-Al_2O_3-coated (e) $Li[Ni_{0.73}Co_{0.12}Mn_{0.15}]O_2$ materials.

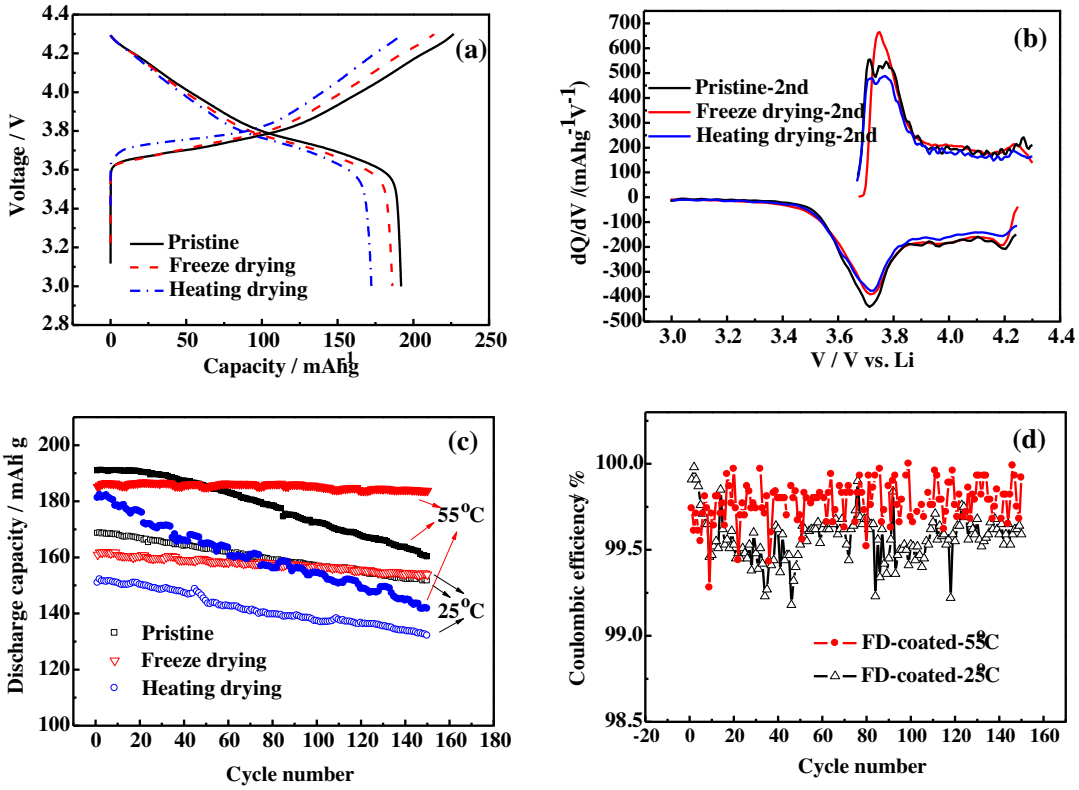

Fig. 4. (a) Initial charge and discharge curves at the current rate of 0.1C, (b) differential capacity vs. voltage curves, (c) cycle performance at the current rate of 1C at 25 °C (hollow) and 55 °C (solid) for the pristine, FD-Al_2O_3-coated and HD-Al_2O_3-coated $Li[Ni_{0.73}Co_{0.12}Mn_{0.15}]O_2$ cathodes between 4.3 and 3.0 V, and (d) coulombic efficiency of FD-Al_2O_3-coated $Li[Ni_{0.73}Co_{0.12}Mn_{0.15}]O_2$ cathodes at 25 °C and 55 °C.

Fig. 4c gives cyclability of the pristine, FD-Al_2O_3-coated and HD-Al_2O_3-coated NCR-CGS $Li[Ni_{0.73}Co_{0.12}Mn_{0.15}]O_2$ electrodes at a current rate of 1 C between 3.0 and 4.3 V at room (25 °C) and elevated (55 °C) temperatures. At room temperature, the pristine $Li[Ni_{0.73}Co_{0.12}Mn_{0.15}]O_2$ electrode shows a steady decrease in capacity throughout the cycling test, leading to a capacity retention of 87.1% after 150 cycles. In contrast, the FD-Al_2O_3-coated $Li[Ni_{0.73}Co_{0.12}Mn_{0.15}]O_2$ electrode is rather stable and presents a remarkably enhanced capacity retention of 95.6% after same cycles. At the elevated temperature, the pristine $Li[Ni_{0.73}Co_{0.12}Mn_{0.15}]O_2$ electrode degrades more rapidly compared with room temperature, which is due to the more severe side reactions between the electrode and the electrolyte at higher temperatures, leading to an increased formation of a nonconducting solid electrolyte interface (SEI) layer and even cell swelling [28]. Nevertheless, as expected, the FD-Al_2O_3-coated $Li[Ni_{0.73}Co_{0.12}Mn_{0.15}]O_2$ electrode exhibits greatly improved cycling performance with a capacity retention of 98.3% after 150 cycles, which is even better than that at room temperature. In comparison, the capacity retention of the HD-Al_2O_3-coated $Li[Ni_{0.73}Co_{0.12}Mn_{0.15}]O_2$ electrode is only 88.4% (25 °C) and 78% (55 °C) after 150 cycles, which is apparently lower than that of the FD-Al_2O_3-coated electrode. The HD-Al_2O_3 coated sample generates some non-active material by the thicker coating layer at some $Li[Ni_{0.73}Co_{0.12}Mn_{0.15}]O_2$ particles, and some non-protection active material at the same time [29,30]. Hence, the capacity and capacity retention of HD-Al_2O_3 coated material are lower than those of other materials. The improvement of cycling stability of FD-Al_2O_3 coated sample at 55 °C may be related to the denser and more stable electrode/electrolyte interface. This interface might be the Li-Al-O layer [31,32], which results from the lithiation of the Al_2O_3 coating layer, or the solid electrolyte interface (SEI) film during charge/discharge cycling. The Li-Al-O layer or SEI film might be denser and more stable at 55 °C, which is revealed by its higher coulombic efficiency than 25 °C demonstrated in Fig. 4d. Therefore, the more stable interface lead to higher capacity retention for FD-Al_2O_3 coated material. These results clearly indicate that the uniform Al_2O_3 coating by freeze drying on the surface of $Li[Ni_{0.73}Co_{0.12}Mn_{0.15}]O_2$ material is very effective at preventing the active material from direct contact with electrolyte, leading to the improved structure stability, the suppressed generation of oxygen and thus significantly enhanced capacity retention [2,33].

Fig. 4 To explore the reason for the significantly enhanced electrochemical stability of the FD-Al_2O_3-coated $Li[Ni_{0.73}Co_{0.12}Mn_{0.15}]O_2$ material, EIS is carried out during the cycling tests. Fig. 5 shows Nyquist plots of the pristine, FD-Al_2O_3-coated and HD-Al_2O_3-coated $Li[Ni_{0.73}Co_{0.12}Mn_{0.15}]O_2$ electrodes at different cycle numbers in the fully charged state. These Nyquist plots present two semicircles in the high and medium frequency regions, respectively. The semicircle at high frequencies is attributed to the resistance of the surface film (*R*sf) that covers on the cathode materials, whereas the semicircle at medium frequencies is associated with the charge transfer resistance (*R*ct) [34,35]. Tables 3 gives the surface film resistance and charge transfer resistance as a function of cycle number for the pristine, FD-Al_2O_3-coated and HD-Al_2O_3-coated $Li[Ni_{0.73}Co_{0.12}Mn_{0.15}]O_2$ electrodes, which are obtained according to the equivalent circuit in Fig. 5. The *R*sf of FD-Al_2O_3-coated $Li[Ni_{0.73}Co_{0.12}Mn_{0.15}]O_2$ materials is consistent with that of pristine sample and HD-Al_2O_3-coated $Li[Ni_{0.73}Co_{0.12}Mn_{0.15}]O_2$ materials. Moreover, the surface film resistance remains small and is kept at very stable values of 15-30 Ω for all the electrodes during cycling. Different from the *R*sf, the *R*ct of the FD-Al_2O_3-coated NRC-CGS $Li[Ni_{0.73}Co_{0.12}Mn_{0.15}]O_2$ electrode maintains relatively stable, while that of pristine and HD-Al_2O_3-coated $Li[Ni_{0.73}Co_{0.12}Mn_{0.15}]O_2$ electrodes rapidly increases along with cycling. Specifically, *R*ct value of the pristine and HD-Al_2O_3-

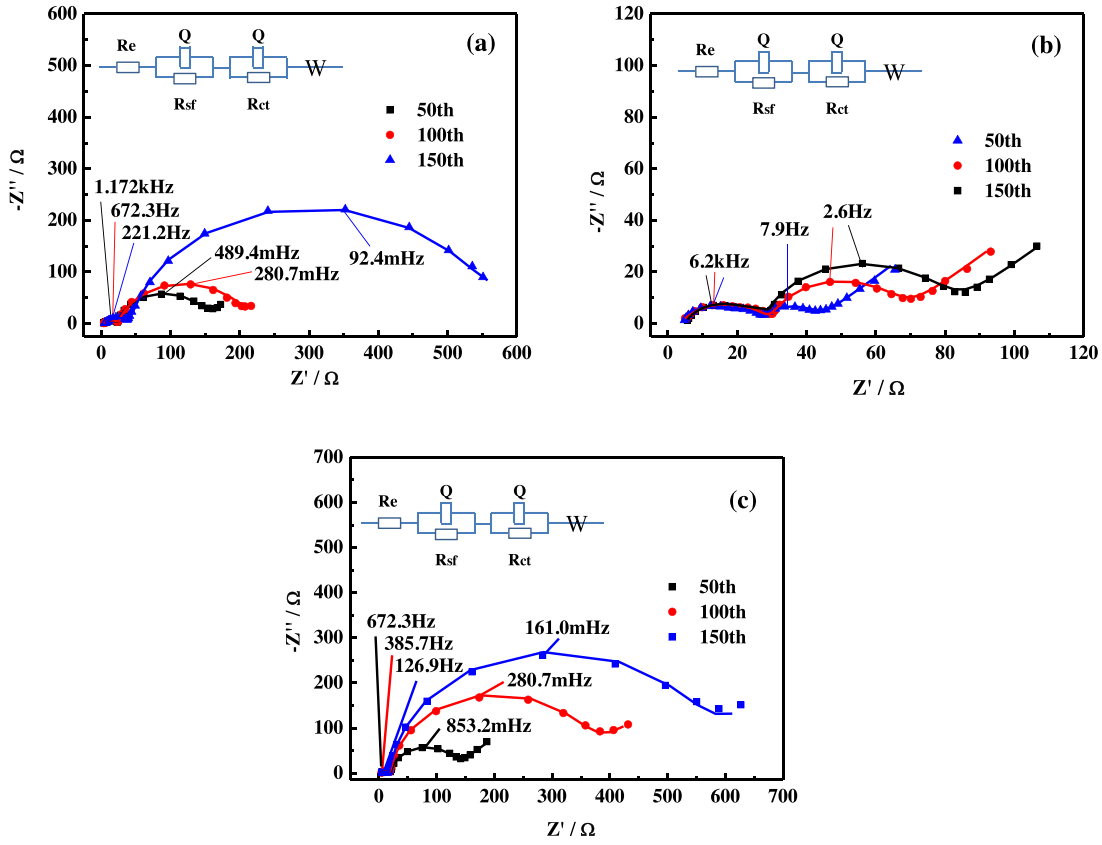

Fig. 5. Experimental (point) and fitted (line) Nyquist plots of the cells with (a) pristine, (b) FD-Al_2O_3-coated and (c) HD-Al_2O_3-coated $LiNi_{0.73}Co_{0.12}Mn_{0.15}O_2$ cathodes at 4.3 V for different cycle numbers. Inset: the equivalent circuit for impedance fitting.

Table 3
Surface film resistance (Rsf) and charge-transfer resistance (Rct) of the pristine, FD-Al_2O_3-coated and HD-Al_2O_3-coated $Li[Ni_{0.73}Co_{0.12}Mn_{0.15}]O_2$ cells for different cycle numbers.

Cycle number	Rsf (Ω)			Rct (Ω)		
	Pristine	Freeze Drying	Heating Drying	Pristine	Freeze Drying	Heating Drying
50th	20.1	21.4	19.3	119.8	20.5	110.2
100th	21.5	25.2	21.9	164.9	34.8	314.7
150th	36.9	22.9	25.5	492.9	48.7	499.1

coated $Li[Ni_{0.73}Co_{0.12}Mn_{0.15}]O_2$ material is 119.8 Ω and 110.2 Ω at the 50th cycle, and drastically increased to 492.9 Ω and 499.1 Ω after 150 cycles. In contrast, *R*ct value of FD-Al_2O_3-coated $Li[Ni_{0.73}Co_{0.12}Mn_{0.15}]O_2$ electrode increases from 20.5 Ω at the 50th cycle to 48.7 Ω at the 150th cycle, which is about 10 times lower than that for the pristine and FD-Al_2O_3-coated $Li[Ni_{0.73}Co_{0.12}Mn_{0.15}]O_2$ electrodes at the 150th cycle. This means that a uniform and stable Al_2O_3 layer on the surface of NRC-CGS $Li[Ni_{0.73}Co_{0.12}Mn_{0.15}]O_2$ material might prevent the interfacial degradation between the electrolyte and cathode material, and limit the increase of charge transfer resistance during cycling, which, in turn, enhances the cycling capability.

4. Conclusions

This paper investigates the effects of the Al_2O_3 coating, which is obtained by a freeze drying method, on the $Li[Ni_{0.73}Co_{0.12}Mn_{0.15}]O_2$ material with a composition of a nickel-rich core and a concentration gradient shell as a cathode material for lithium-ion batteries. A uniform and thin Al_2O_3-coating layer with the thickness of 5 nm is formed on the surface of the $Li[Ni_{0.73}Co_{0.12}Mn_{0.15}]O_2$ material by the freeze drying method. Thus prepared FD-Al_2O_3-coated $Li[Ni_{0.73}Co_{0.12}Mn_{0.15}]O_2$ material shows significantly enhanced cycling performance compared to the pristine and conventional HD-Al_2O_3-coated material. The FD-Al_2O_3-coated $Li[Ni_{0.73}Co_{0.12}Mn_{0.15}]O_2$ material has capacity retention of 98.3%, while the pristine and HD-Al_2O_3-coated materials exhibit a capacity retention of only 84.3% and 78.0%, respectively, after 150 cycles at 55 °C. The improved electrochemical stability of the FD-Al_2O_3-coated $LiNi_{0.73}Co_{0.12}Mn_{0.15}O_2$ material could be ascribed to the protection of the highly deliathiated cathode from being directly contacted with liquid electrolyte by the uniform Al_2O_3 coating layer and the concentration gradient shell. The freeze drying is a promising coating method for the surface modification of electrode materials.

Acknowledgements

This work was financially supported by the National High Technology Research and Development Program of China (863 Program) under Contract No. 2012AA110203, and Applied Technology Research and Development Program of Harbin under Contract No. 2013DB4AP030.

References

[1] M.S. Whittingham, History Evolution, and Future Status of Energy Storage, P. IEEE 100 (2012) 1518.
[2] M. Sathiya, G. Rousse, K. Ramesha, Reversible anionic redox chemistry in high-capacity layered-oxide electrodes, Nat. Mater. 12 (2013) 827.
[3] Y.K. Sun, Z. Chen, H.J. Noh, Nanostructured high-energy cathode materials for advanced lithium batteries, Nat. Mater. 11 (2012) 942.
[4] Y.K. Sun, S.T. Myung, B.C. Park, High-energy cathode material for long-life and safe lithium batteries, Nat. Mater. 8 (2009) 320.

[5] H.J. Noh, S.T. Myung, H.G. Jung, Formation of a Continuous Solid-Solution Particle and its Application to Rechargeable Lithium Batteries, Adv. Funct. Mater. 11 (2012) 942.
[6] Y.K. Sun, D.H. Kim, C.S. Yoon, A Novel Cathode Material with a Concentration-Gradient for High-Energy and Safe Lithium-Ion Batteries, Adv. Funct. Mater. 20 (2010) 485.
[7] Y.S. Jung, P. Lu, A.S. Cavanagh, Unexpected Improved Performance of ALD Coated $LiCoO_2$/Graphite Li-Ion Batteries, Adv. Energy Mater. 3 (2013) 213.
[8] Y.K. Sun, B.R. Lee, H.J. Noh, A novel concentration-gradient Li-$Ni_{0.83}Co_{0.07}Mn_{0.10}O_2$ cathode material for high-energy lithium-ion batteries, J. Mater. Chem. 21 (2011) 10108.
[9] Y.K. Sun, D.H. Kim, H.G. Jung, High-voltage performance of concentration-gradient $Li[Ni_{067}Co_{0.15}Mn_{0.18}]O_2$ cathode material for lithium-ion batteries, Electrochim. Acta 55 (2010) 8621.
[10] X.H. Xiong, Z.X. Wang, G.C. Yan, Role of V_2O_5 coating on $LiNiO_2$-based materials for lithium ion battery, J. Power Sources 245 (2014) 183.
[11] B. Huang, X.H. Li, Z.X. Wang, A comprehensive study on electrochemical performance of Mn-surface-modified $LiNi_{0.8}Co_{0.15}Al_{0.05}O_2$ synthesized by an in situ oxidizing-coating method, J. Power Sources 252 (2014) 200.
[12] E. Jung, Y.J. Park, Suppression of interface reaction of $LiCoO_2$ thin films by Al_2O_3-coating, J. Electroceram. 29 (2012) 23.
[13] Y.S. Jung, A.S. Cavanagh, Y. Yan, Effects of Atomic Layer Deposition of Al_2O_3 on the Li $[Li_{0.20}Mn_{0.54}Ni_{0.13}Co_{0.13}]O_2$ Cathode for Lithium-Ion Batteries, J. Electrochem. Soc. 158 (2011) A1298.
[14] Y.S. Jung, P. Lu, A.S. Cavanagh, Unexpected Improved Performance of ALD Coated $LiCoO_2$/Graphite Li-Ion Batteries, Adv. Energy Mater. 3 (2013) 213.
[15] J.S. Kim, C.S. Johnson, J.T. Vaughey, The Electrochemical Stability of Spinel Electrodes Coated with ZrO_2, Al_2O_3, and SiO_2 from Colloidal Suspensions, J. Electrochem. Soc. 151 (2004) A1755.
[16] H.M. Cheng, F.M. Wang, J.P. Chu, Enhanced Cycleabity in Lithium Ion Batteries: Resulting from Atomic Layer Depostion of Al_2O_3 or TiO_2 on $LiCoO_2$ Electrodes, J. Phys. Chem. C 116 (2012) 7629.
[17] S.B. Park, H.C. Shin, W.G. Lee, Improvement of capacity fading resistance of $LiMn_2O_4$by amphoteric oxides, J. Power Sources 180 (2008) 597.
[18] H.M. Wu, I. Belharouak, A. Abouimrane, Surface modification of $LiNi_{0.5}Mn_{1.5}O_4$ by $ZrP_2O_{\ 7}$ and ZrO_2 for lithium-ion batteries, J. Power Sources 195 (2010) 2909.
[19] Y.L. Ma, Y.Z. Gao, P.J. Zuo, Effect of Sb_2O_3 Modification on Electrochemical Performance of LiMn2O4Cathode Material, Int. J. Electrochem. Sci. 7 (2012) 11001.
[20] W.S. Yoon, W.N. Kyung, D.H. Jang, Structural study of the coating effect on the thermal stability of charged MgO-coated $LiNi_{0.8}Co_{0.2}O_2$ cathodes investigated by in situ XRD, J. Power Sources 217 (2012) 128.
[21] J.C. Arrebola, A. Caballero, L. Hernán, J. Morales, Re-examining the effect of ZnO on nanosized 5V $LiNi_{0.5}Mn_{1.5}O_4$ spinel: An effective procedure for enhancing its rate capability at room and high Temperatures, J. Power Sources 195 (2010) 4278.
[22] I.T. Kim, C.K. James, C. Hugo, Enhanced electrochemical performances of Li-rich layered oxides by surface modification with reduced graphene oxide/$AlPO_4$ hybrid coating, J. Mater. Chem. 2 (2014) 8696.
[23] B.C. Park, H.B. Kim, S.T. Myung, Improvement of structural and electrochemical properties of AlF_3-coated $Li[Ni_{1/3}Co_{1/3}Mn_{1/3}]O_2$ cathode materials on high voltage region, J. Power Sources 178 (2008) 826.
[24] M.H. Eres, D.E. Weidner, L.W. Schwartz, Three-Dimensional Direct Numerical Simulation of Surface-Tension-Gradient Effects on the Leveling of an Evaporating Multicomponent Fluid, Langmuir 15 (1999) 1859.
[25] W. Li, J.N. Reimers, J.R. Dahn, In situ X-ray diffraction and electrochemical studies of $Li_{1-x}NiO_2$, Solid State Ionics 67 (1993) 123.
[26] A.Y. de Dompablo, A. Van der Ven, G. Ceder, First-principles calculations of lithium ordering and phase stability on Li_xNiO_2, Phys. Rev. B 66 (2002) 0641121.
[27] H. Cao, B.J. Xia, Y. Zhang, N.X. Xu, $LiAlO_2$-coated $LiCoO_2$ as cathode material for lithium ion batteries, Solid State Ionics 176 (2005) 911.
[28] K.W. Nam, S.M. Bak, E. Hu, Combining In Situ Synchrotron X-Ray Diffraction and Absorption Techniques with Transmission Electron Microscopy to Study the Origin of Thermal Instability in Overcharged Cathode Materials for Lithium-Ion Batteries, Adv. Funct. Mater. 23 (2012) 1047.
[29] S.T. Myung, K. Izumi, S. Komaba, Role of Alumina Coating on Li-Ni-Co-Mn-O Particles as Positive Electrode Material for Lithium-Ion Batteries, Chem. Mater. 17 (2005) 3695.
[30] L.A. Riley, S. Van Ana, A.S. Cavanagh, Electrochemical effects of ALD surface modification on combustion synthesized $LiNi_{1/3}Mn_{1/3}Co_{1/3}O_2$ as a layered-cathode material[J], J. Power Sources 196 (2011) 3317.
[31] Y. Liu, N.S. Hudak, D.L. Huber, In Situ Transmission Electron Microscopy Observation of Pulverization of Aluminum Nanowires and Evolution of the Thin Surface Al_2O_3 Layers during Lithiation/Delithiation Cycles, Nano Lett. 11 (2011) 4188.
[32] Y. Kim, H.S. Kim, S.W. Martin, Synthesis and electrochemical characteristics of Al_2O_3-coated $LiNi_{1/3}Co_{1/3}Mn_{1/3}O_2$ cathode materials for lithium ion batteries, Electrochim Acta 52 (2006) 1316.
[33] J. Liu, A.J. Manthiram, Functional surface modifications of a high capacity layered $Li[Li_{0.2}Mn_{0.54}Ni_{0.13}Co_{0.13}]O_2$ cathode, J. Mater. Chem. 20 (2010) 3961.
[34] Y.K. Sun, J.M. Han, S.T. Myung, Significant improvement of high voltage cycling behavior AlF_3-coated $LiCoO_2$ cathode, Electrochem. Commun. 8 (2006) 821.
[35] S.U. Woo, C.S. Yoon, K. Amine, I. Belharouak, Y.K. Sun, Significant Improvement of Electrochemical Performance of AlF_3-Coated $LiNi_{0.8}Co_{0.1}Mn_{0.1}O_2$ Cathode Materials, J. Electrochem. Soc. 154 (2007) A1005.